

Modeling of a New Super-Gain BJT and an innovative Low-loss AC Switch based on Gummel-Poon model

Z. Ren, P. Wang, A. Schellmanns, N. Batut and G. Goubard

University of Tours, GREMAN UMR-CNRS 7347, France
7 avenue Marcel Dassault, 37200 Tours (France)
Phone number: +33 6 04 14 70 74, e-mail: zheng.ren@univ-tours.fr

Abstract. This article gives a modeling method based on the Gummel-Poon model for the Super-Gain BJT developed in the GREMAN laboratory. First of all, the extraction principle, mathematical calculating method, and final extraction results of each model parameter will be presented. Secondly, the Gummel and Voltage-Current output curves for a single Super-Gain BJT, which are carried on in Pspice with the extracted parameters in the first part, will be drawn and be compared with experimentation results. At last, a new 600V AC switch that is composed of two single Super-Gain BJTs connected in anti-series is simulated. To explain and reduce the error between the simulated results and experimental ones in hi-level injection, a new model with a dynamic resistance based on that of Gummel-Poon is proposed and validated. Consequently, all of simulations have an error less than 10%, proving the good precision of the models as well as the characteristics of the new AC power switch.

Key words

600V AC Switch, electrical modeling, Gummel-Poon model, Super-Gain BJT, SPICE simulation.

1. Introduction

In power electronics, there are already several types of solutions for AC switch. For example, the Triac, IGBT+diodes and MOSFET+diodes are the common methods used in industry. However, their disadvantages are also obvious. According to the report of GREMAN laboratory [1], three main disadvantages are observed in real applications. The half-controllable problem is found in the Triac, the energy dissipation problem in permanent regime influences the performance of the solution IGBT+diodes and for the latest one, MOSFET+diode [2], which makes the cost of the solution expensive.

In this context, the GREMAN laboratory has proposed a new AC switch named 'TBBS' (Transistor Based Bidirectional Switch) which is based on a Super-Gain (forward amplification gain $h_{FE} > 220$) Gate Associated Bipolar Junction Transistor. This new AC switch is possible to be controlled in both directions and its conduction power dissipation is as low as 0.29W/A compared with others having a magnitude around 1-2W/A [3]. In order to confirm the promising characteristics, electrical simulations have been achieved with the

simulator Pspice. The single Super-Gain BJT and its combined application 'TBBS' are simulated respectively to verify the modeling and test its robustness. The physical structure of the Super-Gain BJT along with equivalent inner diodes and Gummel-Poon model elements are presented in Fig. 1

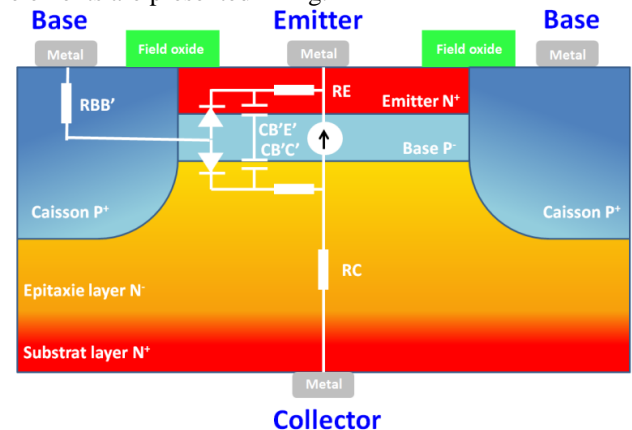


Fig. 1. Physical structure of the Super-Gain BJT along with Gummel-Poon model elements

The TBBS is composed of two Super-Gain BJTs connected in anti-serial, its representative schematic as well as the prototype component is presented as Fig. 2.

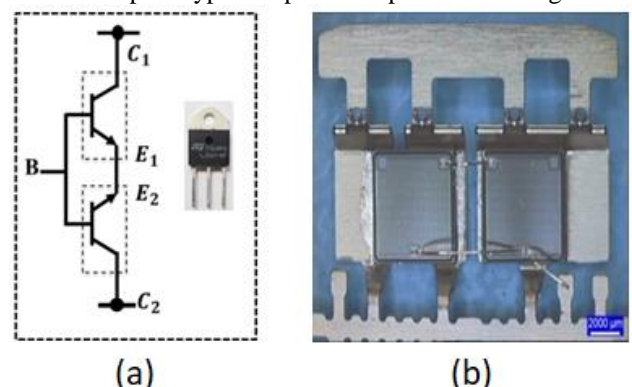


Fig. 2. Representative schematic of the TBBS (a) and the real prototype component (b)

2. The super-gain bjt modeling and the presentation of Gummel-Poon model

As is known, Gummel-poon model was proposed by Hermann Gummel and H. C. Poon in 1970s to simulate

the working principal of bipolar transistor. The model based on the transistor's physical structure is widely used in SPICE simulation software. This article will focus on the extraction of the resistive, capacitive and DC characteristics (forward bias and reverse bias) parameters of the Gummel-Poon model for a Super-Gain BJT.

Before dwelling into the modeling process, some basic mathematical formulas (especially that of Base current i_B and of Collector current i_C) will be given in the following paragraph to help understand how BJT works. The equivalent circuit for a bipolar transistor is presented in Fig.3. In the model, the diodes and the capacitors replace respectively the PN junctions between different layers as well the capacity between terminals. The parasitic resistances, which locate at the end of terminals, are put into operation at high current.

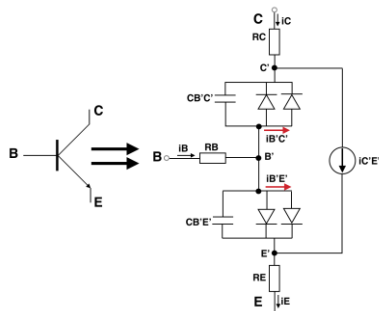


Fig. 3. Gummel-Poon model equivalent electronic circuit for a bipolar transistor

The expression of the base current i_B , which is consisted of 4 independent current parts, is given as follow:

$$i_B = \frac{I_S}{BF} \left\{ \exp \left[\frac{v_{BE}}{NF * vt} \right] - 1 \right\} + I_{se} \left\{ \exp \left[\frac{v_{BE}}{NE * vt} \right] - 1 \right\} + \frac{I_S}{BR} \left\{ \exp \left[\frac{v_{BC}}{NR * vt} \right] - 1 \right\} + I_{sc} \left\{ \exp \left[\frac{v_{BC}}{Nc * vt} \right] - 1 \right\} \quad (1)$$

Similarly, the expression of the collector current i_C :

$$i_C = \frac{I_S}{NqB} * \left\{ \exp \left(\frac{v_{BE}}{NF * vt} \right) - 1 \right\} - \left\{ \exp \left(\frac{v_{BC}}{NR * vt} \right) - 1 \right\} - \frac{I_S}{BR} \left\{ \exp \left(\frac{v_{BC}}{NR * vt} \right) - 1 \right\} - I_{sc} \left\{ \exp \left(\frac{v_{BC}}{Nc * vt} \right) - 1 \right\} \quad (2)$$

3. The parameters extraction of Gummel-Poon model

In this part, the parameters extraction method will be introduced. The extraction process of each type of parameters will be described in detail. In the case of inverse bias, only the differences relative to direct bias will be introduced to avoid repeating the process.

A. Extraction of the resistive parameters

There are three ohmic parameters (R_B , R_C and R_E) in Gummel-Poon model. They represent respectively the resistance of each terminal. The extraction of R_E uses v_{CE} - i_B curve (and v_{EC} - i_B for R_C extraction), here v_{CE} presents the voltage between the electrodes C and E. Its measuring circuit is shown in Fig.4 (keeping i_C equals to 0A, varying the input current i_B and reading the voltage v_{CE} through voltmeter).

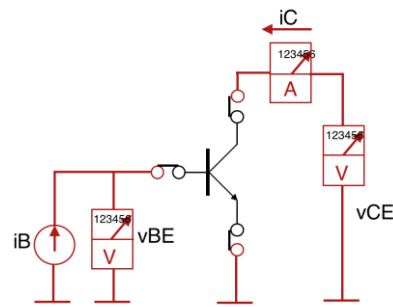


Fig.4 measuring circuit of the resistance R_E (when measuring v_{EC} - i_B , exchange CE probes)

The R_E , R_C represent respectively the emitter and collector access resistances of a transistor. When there is a current flowing through PN junction BE or BC and finally going back to the source, a voltage drop can be detected in another open-loop terminal. Its amplitude is proportional to the base current i_B , which is determined by external drive circuit, and its formula is given as follow:

$$v_{CE} = VT * \ln(1/AI) + i_B * R_E \quad (3)$$

Here AI is the inverse current amplification in common base mode. According to the formula above, to obtain the value of R_E , a simple derivation of variable i_B will be performed in both sides of the equation. For each measured data point of v_{CE} - i_B curve, the derivation result is plotted in the following figure to pick out the value of R_E :

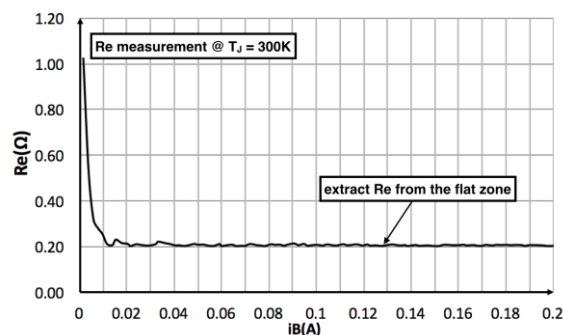


Fig.5 derivation curve of the voltage v_{CE} versus base current i_B

For the ohmic parameters extraction, as the derivation (equivalent to R_E) is a variable of current i_B , its final value should be extracted in the flat zone of the curve as shown in Fig.5. In order to improve the accuracy of parameter extraction and to make it more representative and repeatable, numerous transistors are measured and their ohmic parameters are extracted respectively to calculate finally the average value. The extraction result is given in the following table:

Tab-1: extraction results of resistance R_E and R_C

	Chip-1	Chip-2	Chip-3	Chip-4	Chip-5	Average
$R_E(\Omega)$	0.20	0.19	0.22	0.2	0.19	0.20
$R_C(\Omega)$	0.34	0.35	0.36	0.37	0.33	0.35

B. Extraction of the capacitive parameters

The capacitive parameters used to model the PN junction's capacity of accommodating space charge. The model modeling the capacitances of BE and BC junctions will be introduced in this paragraph.

The extraction of the capacitive parameters requires the use of an instrument called CV meter. This instrument is capable of measuring the ratio of capacitance(C) and voltage (V) between two BJT terminals, all the capacitive parameters extractions are based on these measured data. It will be connected between two chosen electrodes. For example, connecting B and E for Cbe-vBE measurement, and to the opposite, the Cbc-vBE curve is sufficient to connect the CV meter between terminals BC and to keep the rest terminal E 'open'. Combining with the theoretical analysis and the experimentations, the following formulas are used to describe the operation mechanism of space charge between different layers of the super-gain BJT:

For $v_{BE} < F_C * V_{JE}$:

$$C_{SBE} = \frac{C_{JE}}{\left(1 - \frac{v_{BE}}{V_{JE}}\right)^{M_{JE}}} \quad (4)$$

For other cases:

$$C_{SBE} = \frac{C_{JE}}{(1 - F_C)^{(1+M_{JE})}} * \left[1 - F_C * (1 + M_{JE}) + M_{JE} * \frac{v_{BE}}{V_{JE}}\right] \quad (5)$$

The working mechanism of the space charges can be divided into two parts (as shown in Eq.4 and Eq.5), and each of them is determined by the applied voltage. Through Eq.4, the parameter C_{JE} can be easily obtained by fixing $v_{BE}=0V$. The extraction regarding the V_{JE} and M_{JE} relies on Eq.5. After the analysis of this equation and measured curve, the method of linear fitting and parameter identification will be applied to determine the value of these two parameters. From Eq.5, one gets the following expression after transformation:

$$C_{SBE} = \frac{C_{JE}}{(1 - F_C)^{(1+M_{JE})}} * [1 - F_C * (1 + M_{JE})] + \left[\frac{C_{JE}}{(1 - F_C)^{(1+M_{JE})}} * \frac{M_{JE}}{V_{JE}}\right] * v_{BE} \quad (6)$$

It can be observed that **Eq.6** may be considered as a linear function with an independent argument v_{BE} , because other coefficients are constant. Therefore, linear fitting function is constructed as follow:

$$y = b + ax \quad (7-1)$$

$$y = C_{SBE} \quad (7-2)$$

$$b = \frac{C_{JE}}{(1 - F_C)^{(1+M_{JE})}} * [1 - F_C * (1 + M_{JE})] \quad (7-3)$$

$$a = \left[\frac{C_{JE}}{(1 - F_C)^{(1+M_{JE})}} * \frac{M_{JE}}{V_{JE}}\right] \quad (7-4)$$

$$x = v_{BE} \quad (7-5)$$

$F_C = 0.5$ by default. In order to obtain a parameters value more accurate, an interval $0.5V < v_{BE} < 0.8V$ on the C_{je} - v_{BE} curve is defined to extract the remaining two parameter values, V_{JE} and M_{JE} . This specific zone is chosen not only for matching the applying condition ($v_{BE} \geq F_C * V_{JE} \approx 0.5 * 0.6 = 0.3V$), but also for the reason of the highest linearization degree whose R^2 value is close to 1 to reduce the additional error. The fitting result is shown in the following figure:

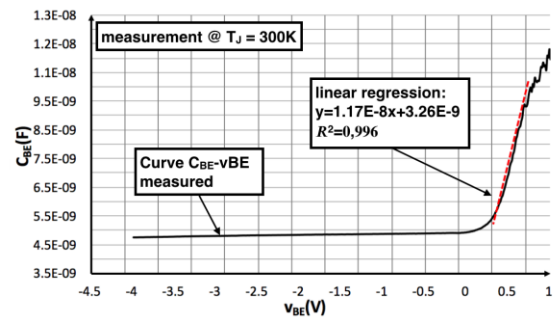


Fig.6 fitting result on the Cbe-vBE curve between $v_{BE}=0.5V$ and $0.8V$

The results for different chips are given as follow:

Tab-3: extraction results of capacitive parameters

	Chip-1	Chip-2	Chip-3	Average
Fitting Equation	$y=1.17E-8x+3.26E-9$ $R^2=0.996$	$y=1.23E-8x+3.408E-9$ $R^2=0.996$	$y=1.35E-8x+3.42E-9$ $R^2=0.993$	
Mje	0.54	0.52	0.52	0.53
Cje(nF)	4.87	4.93	4.97	4.92
Vje(V)	0.65	0.6	0.56	0.6

C. Extraction of the DC parameters

C.1. Extraction of Var and Vaf

The V_{af} and V_{ar} that model transistor's so called 'Early voltage'. They will be the first to be extracted among DC parameters because its dependence with others. The curve i_C - v_{CE} is required for the extraction. According to Fig.4, the curve can be obtained by fixing an input i_B (here is 10, 100 and 100uA), varying the voltage v_{CE} and measuring the collector current i_C . According to Eq.2 given at the beginning, after some simplifications, one can obtain a new i_C expression as follow:

$$i_c = \frac{2 * I_s * \exp\left(\frac{v_{BE}}{NF * VT}\right)}{1 + \sqrt{1 + 4 \frac{I_s}{I_{KF}} \exp\left(\frac{v_{BE}}{NF * VT}\right)}} * \frac{1}{V_{AF}} (V_{AF} + v_{CE}) \quad (8)$$

Referring to this equation, it can be found that parameter V_{af} equals to i_C - v_{CE} curve's intersection with the x-axis. Based on actual operating experience, different i_B values will lead to different V_{af} . It is mainly due to the approximation of some effects during simplification process in Eq.8. Therefore, to obtain a more representative V_{af} value, numerous base current i_B (10uA, 100uA, 1mA) will be selected to compute the Early voltage, the measurement result is 162V. Reverse 'Early voltage' V_{ar} has the same extraction procedure as the forward one. Its measurement result is 5.0V. The V_{af} and V_{ar} will be extracted from each measurement to finally compute their average that is considered as their final value and will be applied in the simulations.

C.2. Extraction of Ise(c), Ne(c) and Bf(r)

Three parameters play a decisive role on the base current i_B . The I_{se} and N_e impact on low current zone of i_B . To the opposite, B_f influences its linear rising segment, which will indirectly impact on the value of the collector current i_C . The extraction of these parameters requires the i_B - v_{BE} curve and its measuring configuration is the

same as that of Is, Nf and Nr extraction. Firstly, according to the expression i_B given in Eq.1, some conditions (v_{BE} around 0.7V and BC junction in reverse bias) are proposed to simplify the computation. Because BC junction in reverse bias, all exponential terms with v_{BC} can be ignored. Practical experience shows that the Is and Ise are nA level parameters, which are ignorable before i_B . Similarly, in order to improve the accuracy, v_{BE} equals to 0.7V indicates that the v_{BE}/V_{AR} can't be ignored compared with 1. In this case, the final base current i_B can be written as:

$$i_B = \frac{1}{BF} * \frac{i_C}{\left(1 - \frac{v_{BE}}{V_{AR}}\right)} + Ise * \exp\left[\frac{v_{BE}}{NE * vt}\right] \quad (9)$$

The extraction of these parameters needs to use the recursive method. Before applying this method, one additional term E_{rel} will be added into Eq.9 representing the error between theoretical value and measurement.

$$E_{rel_i} = \frac{1}{BF * i_{B_i}} * \frac{i_{C_i}}{\left(1 - \frac{v_{BE_i}}{V_{AR}}\right)} + \frac{Ise}{i_{B_i}} * \exp\left[\frac{v_{BE_i}}{NE * vt}\right] - 1 \quad (10)$$

With Eq.10, a new specific function called 'cost function' is proposed as below. 'cost function' is a function that expresses the error between model theory value and actual measurement data. If the 'cost function' gets 0, it means that the model matches perfectly with the measurement.

$$E_{tot} = \sum_{i=1}^N \left[\frac{1}{BF * i_{B_i}} * \frac{i_{C_i}}{\left(1 - \frac{v_{BE_i}}{V_{AR}}\right)} + \frac{Ise}{i_{B_i}} * \exp\left[\frac{v_{BE_i}}{NE * vt}\right] - 1 \right]^2 \quad (11)$$

to be Minimum

Assuming that:

$$i'_{C_i} = \frac{i_{C_i}}{\left(1 - \frac{v_{BE_i}}{V_{AR}}\right)} \quad (12)$$

One calculates the partial derivation of Eq.11 versus Bf and Ise. With the getting derivation results, after simplifications, the Ise can be deduced as follow:

$$\begin{aligned} & \frac{\sum_{i=1}^N \frac{1}{i_{B_i}} \exp\left[\frac{v_{BE_i}}{NE * vt}\right] * \sum_{i=1}^N \frac{i'_{C_i}{}^2}{i_{B_i}^2} - \sum_{i=1}^N \frac{i'_{C_i}}{i_{B_i}} * \sum_{i=1}^N \frac{i'_{C_i}}{i_{B_i}^2} \exp\left[\frac{v_{BE_i}}{NE * vt}\right]}{\sum_{i=1}^N \frac{1}{i_{B_i}^2} \exp\left[\frac{2v_{BE_i}}{NE * vt}\right] * \sum_{i=1}^N \frac{i'_{C_i}{}^2}{i_{B_i}^2} - \left[\sum_{i=1}^N \frac{i'_{C_i}}{i_{B_i}^2} \exp\left[\frac{v_{BE_i}}{NE * vt}\right] \right]^2} \quad (13) \\ & Ise \end{aligned}$$

Similarly, the Bf can be separated to obtain its expression as:

$$BF = \frac{\sum_{i=1}^N \frac{i'_{C_i}{}^2}{i_{B_i}^2}}{\sum_{i=1}^N \frac{i'_{C_i}}{i_{B_i}} - Ise * \sum_{i=1}^N \frac{i'_{C_i}}{i_{B_i}^2} \exp\left[\frac{v_{BE_i}}{NE * vt}\right]} \quad (14)$$

Now it can be observed that only Ne remains unknown in Eq.11. Therefore, a starting value of the Ne will be selected and will be substituted into the Bf and Ise expression. Then, the three parameters (Bf, Ise and Ne) will be substituted together into Eq.11 to compute the value of 'cost function'. One Repeats the above steps and constantly changes the value of Ne until making the 'cost function' the minimum, which means that the theoretical model is the closest to the actual measurements. The average value is calculated as the final model parameter:

Tab-6: extraction results of Ne, Ise and Bf

	Chip-1	Chip-2	Chip-3	Average
Ne	1.967	1.973	1.972	1.971
Ise(A)	1.29E-9	1.33E-9	1.30E-9	1.30E-9
Bf	325	326	323	325

The reverse parameters extraction method is totally the same as that of forward parameters, just be attention at using the curve i_B - v_{BC} instead of the i_B - v_{BE} . After computation, the extraction result is as follow:

Tab-7: extraction results of Nc, Isc and Br

Nc	Isc (A)	Br
1.48	1.36E-9	45

C.3. Extraction of Ikf and Ikr

These parameters present the current roll-off phenomenon when it is high. The extraction of Ikf will use all the parameters that have been extracted previously. So, its extraction process must be very careful to ensure its value in a reasonable range as well as to ensure the success of simulation. The extraction of Ikf needs two groups of measured data: i_C - v_{BE} and i_B - v_{BE} ; the measuring configuration is the same as that used in Is, Nf and Nr extraction.

To simplify the extraction, some conditions (v_{BE} around 0.7v and BC junction in reverse bias) should be respected. The amplification expression of a transistor h_{FE} equals to the ratio of i_C and i_B , which are replaced by their respective mathematic equations to obtain a new amplification expression:

$$h_{FE} = \frac{i_C}{i_B} = \frac{1 - \frac{v_{BE}}{V_{AR}} - \frac{v_{BC}}{V_{AF}} - \frac{i_C}{I_{KF}}}{\frac{1}{BF} + \frac{Ise}{Is} * \exp\left[\frac{v_{BE}}{vt} \left(\frac{1}{NE} - \frac{1}{NF}\right)\right]} \quad (15)$$

In Eq.15, only parameter Ikf is unknown. The same method used in the extraction of Ne, Ise and Bf will be employed again here to identify the value of Ikf. According to the expression of h_{FE} , a new 'cost function' is constructed:

$$E_{tot} = \sum_{i=1}^N \left[\frac{i_{B_i}}{i_{C_i}} * \frac{1 - \frac{v_{BE_i}}{V_{AR}} - \frac{v_{BC_i}}{V_{AF}} - \frac{i_{C_i}}{I_{KF}}}{\frac{1}{BF} + \frac{Ise}{Is} * \exp\left[\frac{v_{BE_i}}{vt} \left(\frac{1}{NE} - \frac{1}{NF}\right)\right]} - 1 \right]^2 \quad (16)$$

→ to be Minimum

The extraction principle is to continuously iterate the new Ikf and to calculate the value of 'cost function' after each iteration until getting its minimum. At this moment, the Ikf gets its optimal value and it also means that the model parameters best meet the actual measurements. The parameter Ikf begins to influence the collector current i_C when its value exceeds a certain intensity. Based on this principle and aimed to make the extraction more reasonable, this article selects the data segment of $v_{BE} \geq 0.7V$ to ensure the collector current i_C working under high intensity.

As shown in Fig.7, after certain iterations, the 'cost function' gets its minimum when the Ikf equals to 13A.

The same extraction method is applied in I_{kr} extraction. According to computation, when I_{kr} equals to 1.75A, the 'cost function' gets the minimum.

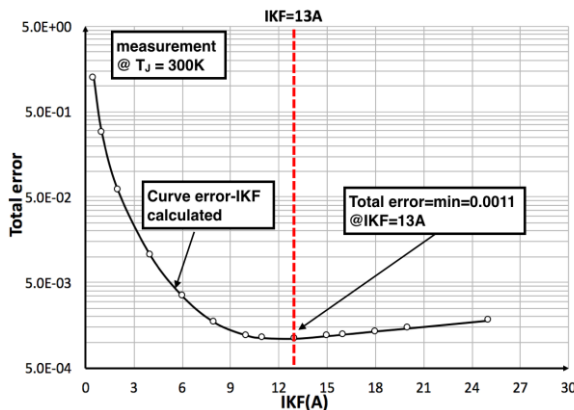


Fig.7 finding the optimal IKF value by doing iteration to make Total error become the minimum

4. The simulation and verification of the model

In the third part, the parameter extraction methods of Gummel-poon model have been introduced one after another. After obtaining all the parameters, in this part, the validation of the model will be performed by comparing the simulation results with experimental ones. The simulation in Pspice will be divided into two parts: simulation of a single Super-Gain BJT and simulation of the TBBS. The simulation results are as follows:

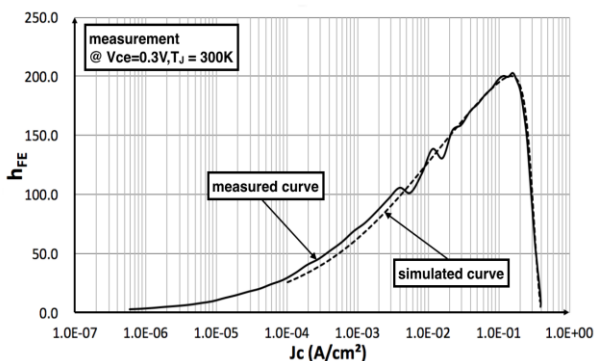


Fig.8 comparison of simulated Gummel curve of a single super-gain BJT with measured one in forward bias

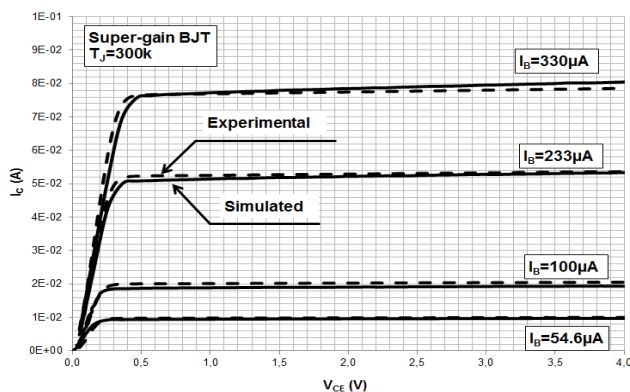


Fig.9 comparison of simulated output curve of a single super-gain BJT with measured one in forward bias

We can observe, for the Gummel curve and output curve of the Super-Gain BJT, that the 'Absolute Total Error'

between the simulated and the measured curve is less than 10%. It proves that the model for the single Super-Gain BJT proposed in this article corresponds completely to its actual electronic characteristics.

5. A new TBBS model and its simulations

In order to establish the TBBS electrical model by using the signal super-gain BJT model, a new Pspice simulation model is proposed. In the new model, two additional resistances R_{cp} and R_{ep} are connected respectively in parallel with the collector terminal C and the emitter terminal E as shown in Fig.10.

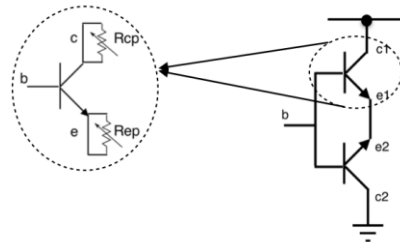


Fig.10 a new TBBS model with two additional resistances

From this paragraph, some simulations based on the new TBBS model will be performed. Before launching the simulations, values of the resistors R_{cp} and R_{ep} should be calculated. By constantly varying their resistances, at each variation, its 'Absolute Total Error' of the Gummel curve should be calculated to find the optimum resistances values that makes the $E_{abs}(tot)$ minimum. Calculating result is as below:

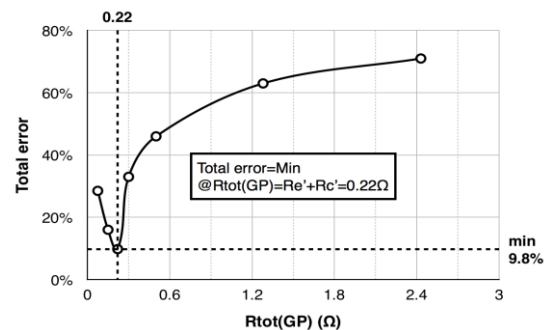


Fig.11 total error curve versus $R_{tot}(GP)$ to find the optimum resistance value making the total error become minimum

According to the calculation, when the $R_{tot}(GP)$ takes 0.22Ω, the Total Error becomes the minimum. In this case, $R_{c'}=0.15\Omega$, $R_{e'}=0.07\Omega$, and the parallel resistors $R_{cp} = 0.262\Omega$, $R_{ep} = 0.108\Omega$. Using the new resistances $R_{c'}=0.15$ and $R_{e'}=0.07\Omega$, the simulation result of TBBS in Pspice is presenting in Fig. 12:

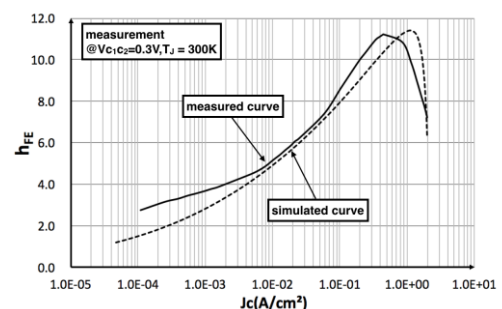


Fig.12 comparison of the simulated Gummel curve with the

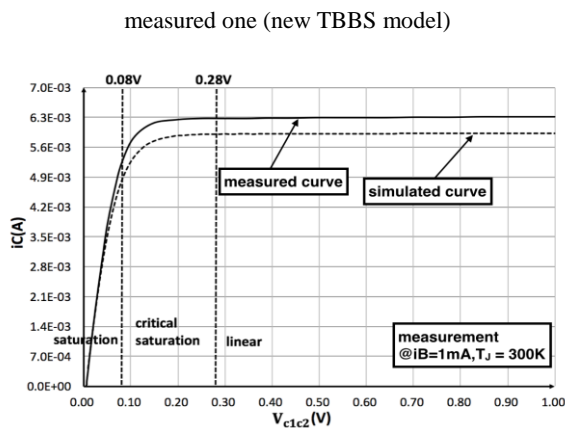


Fig.13 comparison of the simulated output curve with the measured one (new TBBS model)

The absolute total error for the Gummel curve and the output curve are respectively 9.8% and 7.9%, it demonstrates that the new model fits well to the component's electronic characteristics. Thus, its validation is confirmed.

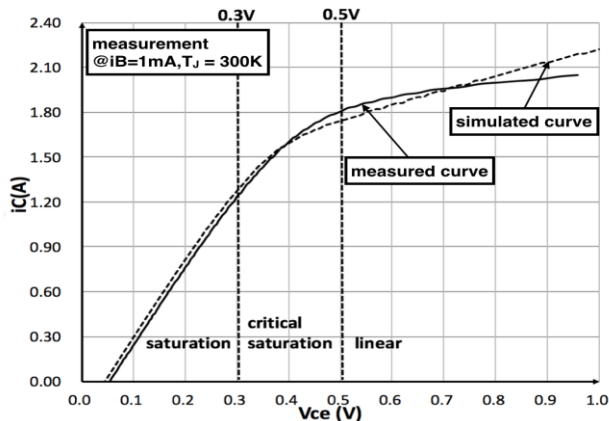


Fig.14 output curve simulation of TBBS in $i_B=500\text{mA}$ with new model

As a new power switch, its collector current i_C will reach in a magnitude of 500mA. Therefore, a new TBBS simulation will be executed in $i_B=500\text{mA}$ to verify its performance in high current and the result is as follow: The Absolute Total Error calculated from the simulation is 3.2% and the simulation parameters are as follows:

Br=45 Ikr=1.75A Nc=1.48, Nr=1.05, Isc=1.36n, Var=5,
Is=0.13n Ise=1.3n Ne=1.95 Nf=1.053 Bf=325 Vaf=162
Mje=0.53 Cje=4.92E-9 Vje=0.60 Mjc=0.32 Cjc=0.92E-9
Vjc=0.53 Ikf=13 Re=0.035 Rc=0.04 Rb=3.022

6. Conclusion and prospective

On the basis of the research of the new Super-Gain BJT developed by laboratory GREMAN, this article introduces in a detailed method for modeling the Super-Gain BJT and of extracting its model parameters. Simultaneously, the single BJT and the power switch TBBS (two Super-Gain BJTs connected in anti-series) are simulated in Pspice to validate their electrical models. According to the simulation results, a new TBBS simulation model and its interpretation is given to overcome the defect of Gummel-Poon model. Consequently, in all simulation cases, the

'Absolute Total Error' is less than 10%, it fully proves that the model used in this article and its extracted parameters are correct.

It is a great challenge to simulate the Super-Gain BJT with Gummel-Poon model in hi-level injection. The simulation result from Pspice indicates that the proposed model becomes more erroneous when current density J_c is higher than $2.0 \text{ (A/cm}^2\text{)}$ principally due to the influence of resistances. To extend the validation scope to a larger one, furthermore, researchers should focus on modeling the high-current injection part of Super-Gain BJT. Against the shortcoming of Gummel-Poon model, we propose an efficient modified method to improve its performance in modeling the Super-Gain BJT. That is replacing the fixed-value resistance by a current-depend resistance in the model for the aim of simulating the resistance effect and of making up for deficiencies of Gummel-Poon model. This resistance will change its value according to the current flowing through it and definitively make the simulations more flexible and more accurate. The simulation results of this new model have proved its robustness.

REFERENCES

- [1] C. Benboujema, S. Jacques, A. Schellmanns, N. Batut, J.-B. Quoirin, L. Jaouen, L. Ventura, Characterization of a high gain BJT used in power conversion on AC mains, Proceedings of the IEEE Energy Conversion Congress and Exposition, 2010, pp. 357-361.
- [2] Rectifier and controller including triac switch. U.S. Patent No 3,421,063, 7 janv. 1969.
- [3] Hefner, A. R. (1990, June). An investigation of the drive circuit requirements for the power insulated gate bipolar transistor (IGBT). In Power Electronics Specialists Conference, 1990. PESC'90 Record., 21st Annual IEEE (pp. 126-137). IEEE.
- [4] Lundstrom, M. (1997). Elementary scattering theory of the Si MOSFET. IEEE Electron Device Letters, 18(7), 361-363.
- [5] Holtz, J., Lammert, P., & Lotzkat, W. (1987). High-speed drive system with ultrasonic MOSFET PWM inverter and single-chip microprocessor control. IEEE transactions on industry applications, (6), 1010-1015.
- [6] REN Zheng, SCHELLMANNNS Ambroise, BATUT Nathalie, "Development and Static Mode Characterization of a New Low-loss AC Switch Based on Super-Gain BJT", Special issue published in Journal of Energy and Power Engineering in January 2014.
- [7] L.-V. Phung, Chawki Benboujema, Jean-Baptiste Quoirin, BATUT Nathalie, Modeling of a new SOI bidirectional bipolar junction transistor for low-loss household appliances, IEEE Transactions on Electron Devices, Vol. 58, No 4, 2011, pp. 1164-1169.
- [8] REN Zheng, SCHELLMANNNS Ambroise, BATUT Nathalie. Dynamic Mode Characterization of a New Super-Gain BJT and an Innovative Low-Loss AC Switch. In: 2016 IEEE Workshop on Microelectronics and Electron Devices (WMED). IEEE, 2016. p. 1-4.
- [9] Franz Sischka, "Gummel-Poon Bipolar Model, model description and parameter extraction", Agilent Technologies GmbH, 2006, Munich (Germany)